

Simulation and validation of the ATLAS Tile Calorimeter response

S.N. Karpov^{*} on behalf of the ATLAS Collaboration

*Joint Institute for Nuclear Research,
Joliot-Curie 6, Dubna, Moscow region, 141980, Russia*
E-mail: Sergey.Karpov@cern.ch

ABSTRACT: The Tile Calorimeter is the central section of the ATLAS hadronic calorimeter at the Large Hadron Collider. Scintillation light produced in the tiles is transmitted by wavelength shifting fibers to photomultiplier tubes (PMTs). The resulting electronic signals from approximately 10000 PMTs are amplified, shaped and digitized before being transferred to off-detector data acquisition systems. This paper describes the detailed simulation of this large scale calorimeter from the implementation of the geometrical elements down to the realistic description of the electronics readout pulses, the special noise treatment and the signal reconstruction. The recently improved description of the optical and electronic signal propagation is highlighted and the validation with the real particle data is presented.

KEYWORDS: Calorimeter; Response; Simulation; Validation.



^{*} Corresponding author.

Contents

1. The ATLAS Tile Calorimeter	1
2. Simulation of the ATLAS Tile Calorimeter	1
2.1 Tile Calorimeter simulations with calibration hits	2
2.2 Cell response as function of the particle impact point	2
2.3 Sampling fraction calculation	4
3. Validation of the Tile Calorimeter response	5
3.1 Validation of EM scale with muons in ATLAS	5
3.2 Electronic Noise	6
3.3 Noise with pileup	6
4. Conclusion	7
References	7

1. The ATLAS Tile Calorimeter

The Tile Calorimeter (TileCal) [1] is the central section of hadronic calorimeter of the ATLAS experiment [2] at the Large Hadron Collider [3]. The total length is 12 m and the diameter is 8.5 m. There are 3 cylindrical sections: Long Barrel and two Extended Barrels. Each barrel is divided in 64 modules in ϕ . The module consists of alternating layers of steel absorber and scintillating tiles. The cell granularity is $\Delta\eta \times \Delta\phi = 0.1 \times 0.1$ (0.2×0.1 in the outermost radial sample D). The granularity corresponds to trigger towers of the calorimeters. There are over 5000 cells in total. Each scintillating tile is being read by two photomultiplier tubes (PMTs) from either side of the cell (except for some special cells) via wavelength shifting fibers.

The cell energy is the sum of the energy measured in the two channels. The design resolution of TileCal for jets is: $\sigma_E/E = 50\% / \sqrt{E} \oplus 3\%$, E in GeV [4]. The double readout reduces the dependence on the light attenuation in the scintillator and improves the response uniformity. The readout electronics (including the PMTs) is located at the outer radius of the calorimeter (inside the girder). The total thickness of TileCal is $7.4 \lambda_{\text{int}}$ at $\eta=0$. Three radial samplings A, BC, D correspond to 1.5, 4.1, $1.8 \lambda_{\text{int}}$ in the Long Barrel and 1.5, 2.6, $3.3 \lambda_{\text{int}}$ in the Extended Barrel. TileCal covers the pseudo-rapidity region $|\eta| < 1.7$.

2. Simulation of the ATLAS Tile Calorimeter

In a Geant4 simulation the passage of particles through the ATLAS detector is characterized by hits. Each hit is defined by the energy deposition, its position and time. We have only information from the sensitive material of the detector from the real experiment. The sensitive part of the TileCal is the scintillator and therefore Birk saturation law must be applied to every

Geant4 hit before adding this hit energy to the total energy. When the simulation is finished (the hits are collected and stored), the next step is the digitization.

Simulation of cosmic muons is slightly different from simulation of pp collisions. In particular, the internal time of Geant4 hits in the calorimeter can be an arbitrary value – not a few nanoseconds, but hundreds of nanoseconds. It is the arrival time of muons passing from the earth surface to the detector in the pit. And special precautions have to be made in order to collect and to reconstruct those hits properly.

The η , ϕ and radial segmentation define the three dimensional cells in TileCal. The geometry of TileCal is not completely symmetric relative to interaction point along z (beam axis) and in ϕ direction. A few cells have a special shape, asymmetric inactive material etc. All currently known geometric details are carefully described in the MC geometry model.

2.1 Tile Calorimeter simulations with calibration hits

Calibration hits allow us to record not only the energy deposited in the scintillator, but also in the non-sensitive parts of TileCal. The energy of the event is divided in electromagnetic, non-electromagnetic, invisible (neutrino) and escaping (leakage energy) components. By definition the sampling calorimeter consists of *active* and *inactive materials*, but material of support such as: saddle, girder and extra iron structures at outer radius of the calorimeter, readout electronics inside the girder, cables, and other services are called *dead material*.

The calibration hits give us very useful information for the energy calibration studies: calibration of each ATLAS sub-detector and verification of its geometry; understanding of the full energy balance of specific event types, for example evaluation of "missing visible energy" which can be caused by energy deposits in dead materials, by leakage, or by energy flow at $|\eta| > 5.9$; identification of the full energy which is associated with each jet in multi-jet events. The calibration hits are also used in the determination of the PMT response as a function of the coordinates of the energy deposition point (U-shape) and the *sampling fraction* determination.

It is also possible to simulate the TileCal standalone Test Beams (3 barrel modules or 2 barrels and 2 extended barrels) as well as the Combined Test Beam of 2004 [5]. This is particularly useful for the *sampling fraction* calculation.

2.2 Cell response as function of the particle impact point

The dependence of the scintillating tile response to the particle impact point (U-shape) is obtained in measurement of the $\langle dE/dx \rangle$ value of muons produced in leptonic decays of $W \rightarrow \mu\nu$. They are represented in Figure 1 [6]. $\Delta\phi$ is the azimuthal angle difference between the muon track impact point on the cell and the center of the cell. The profiles were obtained for the cells of the three radial layers of the TileCal Long end Extended Barrels. The criteria are applied to select well reconstructed tracks and to select $W \rightarrow \mu\nu$ events: exactly one muon, $p_{T\mu} > 15$ GeV, transverse mass $M_T > 40$ GeV, missing $E_T > 25$ GeV, $p_T < 1$ GeV in a cone of $\Delta R = \Delta\eta \times \Delta\phi = 0.4$ around track, $E_{LAr} < 3$ GeV in a cone of $\Delta R = 0.4$, $20 < p_\mu < 100$ GeV, the energy deposited in the cell $\Delta E > 60$ MeV and the path length of muon in the cell $\Delta x > 15$ cm.

The response correction factor for each PMT was estimated as the ratio of the $\langle dE/dx \rangle$ for single PMT from the collision data at $\sqrt{s} = 8$ TeV divided by $\langle dE/dx \rangle$ using total energy deposited in the cell in simulation without U-shape. Muons from the $W \rightarrow \mu\nu$ events were used in the data and single projective muons distributed uniformly in the ATLAS detector were used in simulation. The dependence of the response correction factor over $\Delta\phi$ for A-layer cells of the

Long Barrel is shown in [Figure 2](#), left panel [\[6\]](#). The non-linear form of the dependence originates from the non-uniformity of the light yield over the volume of the scintillating tiles.

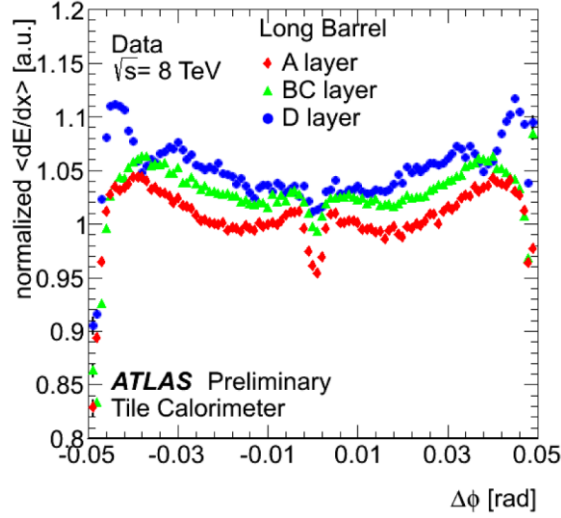


Figure 1. The dependence of the scintillating tiles response on the particle impact point (U-shape) for the A, BC and D layers of the Long Barrel of TileCal. The $\langle dE/dx \rangle$ value is obtained from muons produced in leptonic decays of $W \rightarrow \mu\nu$. $\Delta\phi$ is the azimuthal angle difference between the muon track impact point on the cell and the center of the cell.

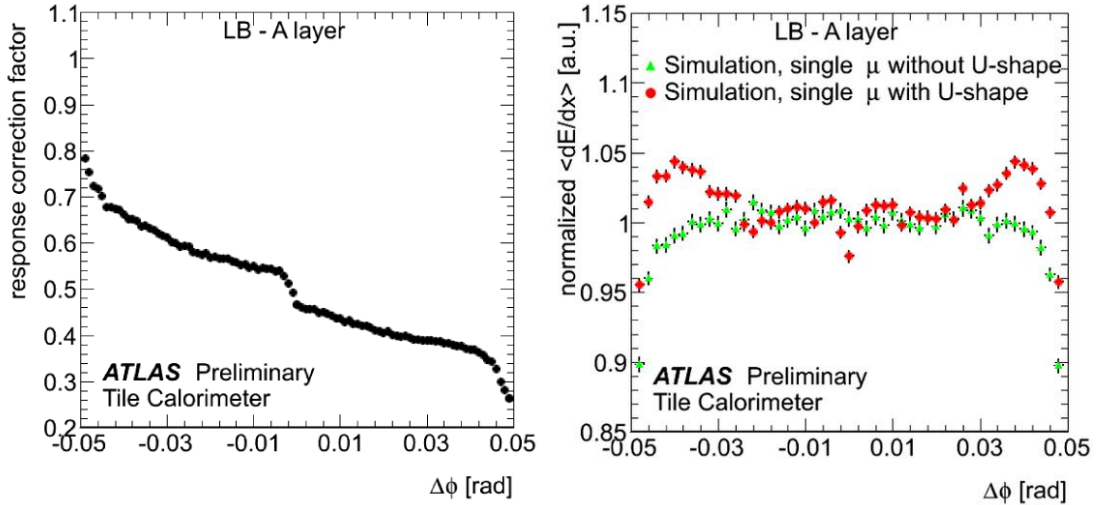


Figure 2. The dependence of the response correction factor over $\Delta\phi$ for A-layer cells of the Long Barrel (left panel) and the normalized $\langle dE/dx \rangle$ distributions obtained with (without) U-shape in the MC simulation (right panel).

Correction factors for channels (PMTs) organized in *look-up tables* (LUTs). Nine LUTs have been derived and used in the simulation to correct for the energy in the cells: 3 radial samplings for the Long Barrel, 3 radial samplings for each Extended Barrel. Each LUT contains 99 points for the $\Delta\phi$ range $[-0.0495, 0.0495]$. The LUTs for two PMTs in a cell are symmetric: $LUT_{PMT1}(\Delta\phi) = LUT_{PMT2}(-\Delta\phi)$. Moreover, the LUTs are scaled twice: 1) the average value in every LUT for one PMT is set to 0.5; 2) all LUTs are rescaled to have the same *sampling*

fraction for 100 GeV electrons at $\eta = 0.35$ in the center of the cell (Test Beam simulation with beam width = 40 mm). The LUTs are now applied to each PMT in all barrels and radial layers of TileCal in the ATLAS full simulation. First the standard Geant4 simulation is carried out for particles passing through the TileCal and then the energy computed by Geant4 for a given cell is corrected using the LUT.

The red (green) dots distributions in [Figure 2](#) (right) [\[6\]](#) were obtained with (without) U-shape in the MC simulation. An up to 6% difference between simulation with and without U-shape is observed in the Long Barrel, A-layer. This can reach 10% in other layers and barrels. However, the $\langle dE/dx \rangle$ of muons from the $W \rightarrow \mu\nu$ events for the collision data ([Figure 1](#), red) agrees very well (within 1%) with simulation with U-shape included ([Figure 2](#), right, red).

2.3 Sampling fraction calculation

The *sampling fraction* (SF) is the conversion factor between the energy released in the scintillators and the total energy deposited in the TileCal cells. The total deposited energy is equal to the beam energy E_{beam} in the Test Beam case (data or MC simulation). The energy in outputs from the ordinary simulations (at hit level) is equal to energy released in the active material (E_{sci}). The cell energy is then calculated as the energy in the scintillators multiplied by a constant value $1/\text{SF}$. If the invisible energy and energy leakage are neglected, the *sampling fraction* is $E_{\text{beam}}/E_{\text{sci}} = 1/\text{SF}$.

Single particles in the Test Beam setup were simulated to obtain the dependence of SF over η . Electron beams at 5, 20 and 100 GeV were simulated in an η -projective geometry ($0.05 < |\eta| < 0.85$). SF for 100 GeV electron beam is shown in [Figure 3](#) [\[7\]](#).

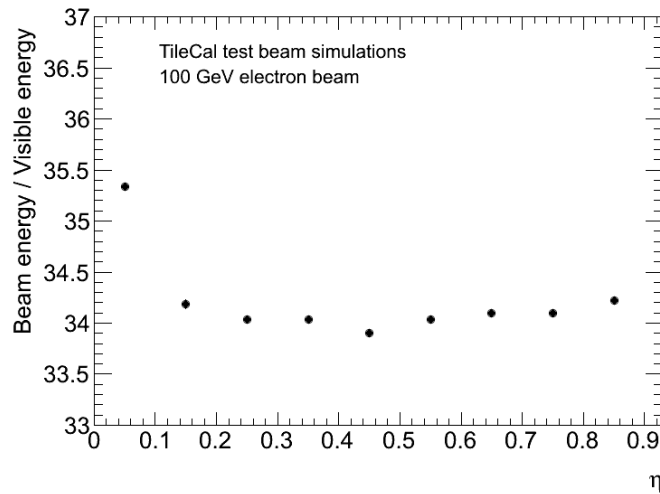


Figure 3. The dependence of the TileCal sampling fraction over η obtained with full Geant4 simulation of a 100 GeV electron beam.

The *sampling fraction* is almost constant in the pseudo-rapidity region between 0.15 and 0.85. The increase of the $1/\text{SF}$ at small $\eta = 0.05$, i.e. decrease of the energy deposit in the scintillator, can be qualitatively explained by the periodic scintillator/iron structure of the TileCal: the narrow EM shower at low angle can touch only one scintillator and two neighbor iron plate.

The single electron samples were also simulated at 90 degrees to the module. The $1/\text{SF}$ values for electron beams at 5, 20 and 100 GeV at various values of η are in the [Table 1](#).

E_{beam} [GeV]	η : 0.25–0.75	90 degrees
5	34.341 ± 0.018	33.934 ± 0.019
20	34.140 ± 0.011	33.494 ± 0.009
100	34.045 ± 0.005	33.356 ± 0.004

Table 1. The TileCal sampling fraction for various E_{beam} and η .

The value of $1/\text{SF}$ depends slightly on energy. The maximum of the EM shower is shifted to higher depth at higher beam energy. The energy fraction released in the iron front plate of the TileCal becomes smaller and the energy fraction released in scintillator increases somewhat. The systematic error in $1/\text{SF}$ obtained in the MC simulation is 0.8%.

The TileCal MC simulation uses a constant $1/\text{SF} = 34.0$, which is the sampling fraction at $\eta = 0.35$. This is also the pseudo-rapidity of the test beam where the electromagnetic scale in TileCal was defined.

3. Validation of the Tile Calorimeter response

3.1 Validation of EM scale with muons in ATLAS

The example of the muon signal and corresponding noise is represented in [Figure 4](#) (left) [\[4\]](#) for projective cosmic muons entering the barrel modules at $0.3 < |\eta| < 0.4$. The total energy summed up over the last radial layer of TileCal (D-layer) that can possibly be eventually used to assist the muon identification. The signal (red) comes from the cosmic muon data sample, the corresponding noise (black) is obtained from the random trigger sample.

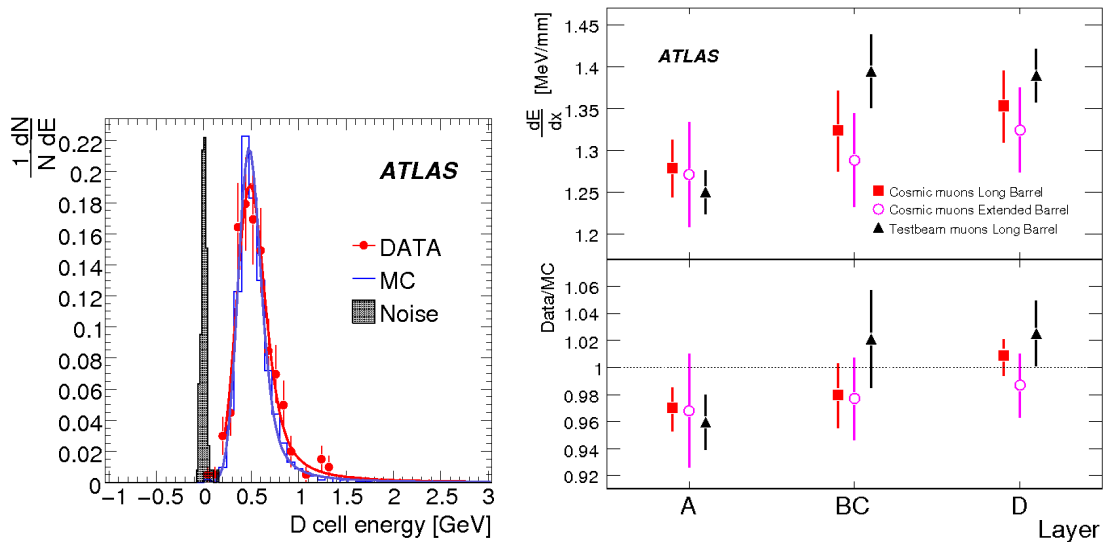


Figure 4. The muon signal, corresponding noise and $\langle dE/dx \rangle$ for cosmic and test beam muons in various TileCal layers.

The $\langle dE/dx \rangle$ values for cosmic muons and the Test Beam muons are shown in [Figure 4](#) (right) [\[4\]](#) per radial layer and they are compared to Monte Carlo at the bottom. For the cosmic muon

data, the results were obtained for modules at the bottom part of the calorimeter. The error bars shown combine both statistical and systematic uncertainty summed in quadrature. The results show that reconstructed dE/dx for MC and data are compatible to a level a few percents.

3.2 Electronic Noise

The electronic noise in TileCal is not Gaussian as one can see in [Figure 5](#) (left) [\[8\]](#). It can be approximated with two Gaussians. Mainly, such shape comes from the Low Voltage Power Supply (LVPS) providing power for front-end electronics. A comparison was made between the reconstructed energy in 100k events of two high statistics pedestal runs (run 192130 – 2011 and run 195843 – 2012), for module LBC41, channel 47, a previously very noisy channel. The reconstruction of energy in the events is performed using the Non-iterative Optimal Filtering method. LBC41 had its LVPS changed from version 6.5.4 to version 7.5 in winter 2011-2012. The RMS of the noise distribution for the channel goes down by almost a factor of 2 after changing LVPS. Both noise cases are implemented in Monte Carlo. After the LHC shutdown in 2013-2014, all modules are equipped with new LVPS showing almost perfect Gaussian noise and improved correlated noise as well.

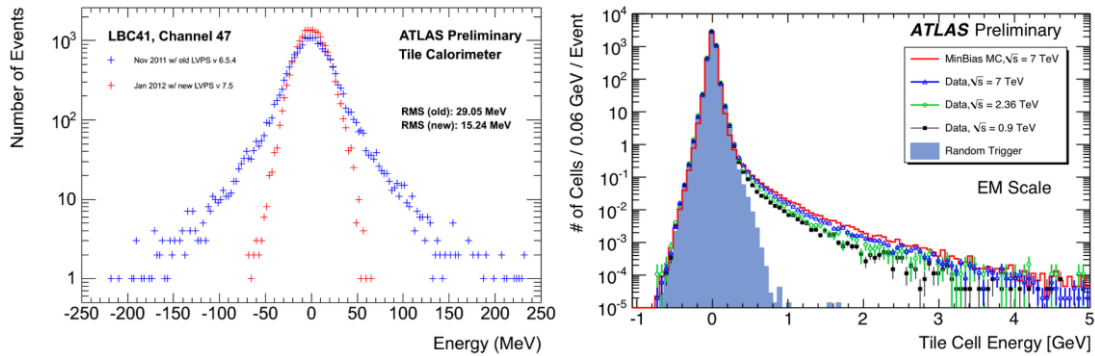


Figure 5. The electronic noise in a TileCal module with old and new LVPS (left) and the energy distributions of the TileCal cells in comparison with Monte Carlo (right).

The energy of the TileCal cells is shown in [Figure 5](#) (right) [\[9\]](#). Here the distributions from collision data at 7 TeV, 2.36 TeV, and 0.9 TeV are superimposed with Pythia minimum bias Monte Carlo and randomly triggered events. Each distribution is normalized with the number of events. The negative side demonstrates good agreement with the MC noise simulation using the double Gaussian description.

3.3 Noise with pileup

A realistic description of the total noise (Electronic and Pileup noise summed in quadrature) is mandatory for the calorimeter triggers [\[10\]](#) and jet energy reconstruction [\[11\]](#). The total noise distributions of different Tilecal cells as a function of $|\eta|$ are represented in [Figure 6](#) [\[12\]](#).

Pileup is characterized by the average number of minimum bias collisions ($\langle\mu\rangle$) overlaid on a hard scattering event. The distributions were obtained for the zero bias run 216416 of 2012 at a centre-of-mass energy of 8 TeV with a bunch spacing $\Delta T = 25$ ns and an average number of interactions $\langle\mu\rangle = 10.0$ per bunch crossing. The Monte Carlo simulation was reweighted to the average number of interactions in data. The noise was estimated as the standard deviation of the measured cell energy distribution. The histograms show the results obtained for cells from

different layers in TileCal (A, BC, D and Special Cells). Overall, the difference between noise in data and in the MC simulation is not more than 20%.

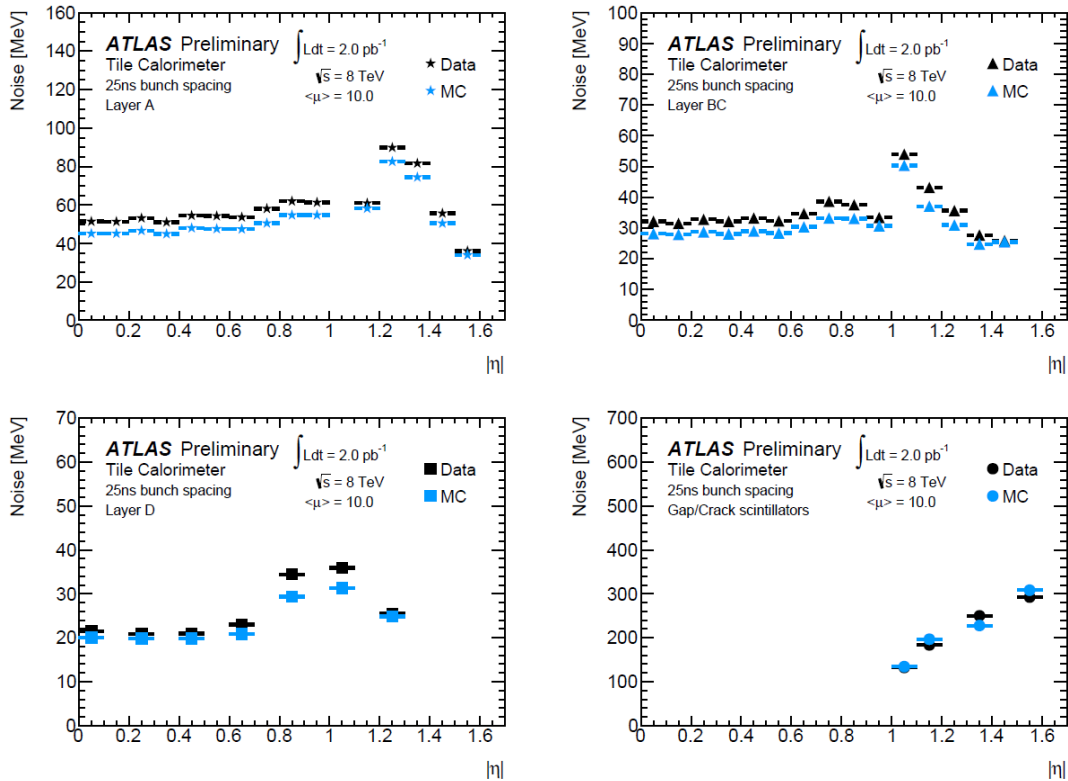


Figure 6. The comparison of the noise distribution with pileup as a function of $|\eta|$ in the collision data and in MC simulation for different TileCal cells: layer A – top and left panel, layer BC – top and right, layer D – bottom and left, Special Cells – bottom and right.

4. Conclusion

The detailed simulation of the Tile Calorimeter and the precise implementation of the detector characteristics for the ATLAS environment led to a very good description of the TileCal response. The simulation with calibration hits is very useful for the energy calibration studies, verification of the ATLAS geometry, determination of the PMT response and the *sampling fraction*. The PMT response with U-shape correction is more precise and can have some effect on MC systematics. The *sampling fraction* calculation is in good conformity with earlier Test Beam measurements. The thorough validation of the Tile Calorimeter simulation shows in particular a good description of the muon energy deposition. Models for both electronic noise and pileup noise are implemented in Monte Carlo, and show good agreement with data. A solid basis for the full simulation of Tile Calorimeter and ATLAS was achieved.

References

- [1] ATLAS Collaboration, *Tile Calorimeter Technical Design Report*, CERN, Geneva, Switzerland, [CERN-LHCC-96-42](#), 1996.

- [2] ATLAS Collaboration, *The ATLAS Experiment at the CERN Large Hadron Collider*, [JINST 3 \(2008\) S08003](#).
- [3] L. Evans and P. Bryant (editors), *LHC Machine*, [JINST 3 \(2008\) S08001](#).
- [4] ATLAS Collaboration, *Readiness of the ATLAS Tile Calorimeter for LHC collisions*, [Eur. Phys. J. C 70 \(2010\) 1193](#).
- [5] E. Abat et al., *Study of energy response and resolution of the ATLAS barrel calorimeter to hadrons of energies from 20 to 350 GeV*, [NIM A 621 \(2010\) 134](#).
- [6] ATLAS Collaboration, *Approved Plots and Public Results, Tile Calorimeter, U-shape*, https://twiki.cern.ch/twiki/bin/view/AtlasPublic/TileCaloPublicResults#U_shape
- [7] ATLAS Collaboration, *Approved Plots and Public Results, Tile Calorimeter, Sampling fraction*, https://twiki.cern.ch/twiki/bin/view/AtlasPublic/ApprovedPlotsTile#Sampling_fraction
- [8] ATLAS Collaboration, *Approved Plots and Public Results, Tile Calorimeter, Noise characteristics*, https://twiki.cern.ch/twiki/bin/view/AtlasPublic/ApprovedPlotsTileNoise#Noise_characteristics
- [9] ATLAS Collaboration, *Approved Plots and Public Results, Tile Calorimeter, Energy deposition*, https://twiki.cern.ch/twiki/bin/view/AtlasPublic/TileCaloPublicResults#Energy_deposition
- [10] ATLAS Collaboration, *Performance of the ATLAS Trigger System in 2010*, [Eur. Phys. J. C 72 \(2012\) 1849](#)
- [11] ATLAS Collaboration, *Jet energy measurement with the ATLAS detector in proton-proton collisions at $\sqrt{s} = 7$ TeV*, [Eur. Phys. J. C 73 \(2013\) 2304](#)
- [12] ATLAS Collaboration, *Approved Plots and Public Results, Tile Calorimeter, Pile-up Noise*, https://twiki.cern.ch/twiki/bin/view/AtlasPublic/ApprovedPlotsTileNoise#Pile_up_Noise_2012